Thermodynamic and Transport Properties of the $PrBr_3$−KBr Binary System†

Joanna Rejek,‡ Leszek Rycerz,‡ Ewa Ingier-Stocka,‡ and Marcelle Gaune-Escard*,§

Chemical Metallurgy Group, Faculty of Chemistry, Wroclaw University of Technology, Wybrzeze Wyspianskiego 27, 50-370 Wroclaw, Poland, and Ecole Polytechnique, IUSTI CNRS UMR 6595, Technopole de Chateau-Gombert, 5 rue Enrico Fermi, 13453 Marseille Cedex 13, France

Phase equilibrium in the $PrBr_3$−KBr binary system was established from differential scanning calorimetry (DSC). This system exhibits three compounds, K_3PrBr_6, K_2PrBr_5, and KPr_2Br_7, and two eutectics located at a mole fraction of $PrBr_3$ ($x = 0.182$; 849 K and $x = 0.552$; 753 K), respectively. K_3PrBr_6 forms at 727 K and melts congruently at 904 K. K_2PrBr_5 melts incongruently at 847 K, and finally KPr_2Br_7 forms at 697 K and melts incongruently at 786 K. The electrical conductivity of $PrBr_3$−KBr liquid mixtures was measured down to temperatures below solidification over the whole composition range. Results obtained are discussed in terms of possible complex formation.

Introduction

Rare-earth halides are technologically important since they are used in a number of applications like reprocessing of nuclear wastes, recycling of spent nuclear fuel, doses in high-intensity discharge lamps, new highly efficient light sources with energy-saving features, lasers, and so forth. However, we observed previously[1] that they have been poorly characterized until recently. The phase diagrams of the $MX-LnX_3$ (lanthanide halide + alkali metal halide) binary systems available in literature very often either contain serious errors or lack precision.[1] This situation was the trigger to a systematic investigation program on these systems to determine their thermodynamic structure and electrical conductivity properties, using several complementary experimental techniques. All of the lanthanide/alkali metal chloride binary systems have been successfully examined or reexamined by Seifert.[2] The phase diagrams of the homologous bromide and iodide systems were not fully investigated nor critically assessed yet. Some lanthanide−alkali metal bromide systems seem totally erroneous: for the $TmBr_3$−RbBr system,[3] for instance, no congruently melting compound has been reported, while at least one congruently melting compound was to be foreseen by analogy to the huge number of similar systems. Other systems were investigated,[4] but the data obtained have been given as graphic-only information. Moreover, no compositional or temperature values for invariant points were provided by the authors. Therefore, it is clear that more details are required to fully characterize those systems. In view of the above discrepancies or lack of data for many $LnBr_3$-based binary systems, we decided to assess existing data and to investigate the still unexplored lanthanide bromide-based systems.

The present paper is a part of our ongoing extensive program focused on thermodynamic properties, structure, and electrical conductivity of $MX-LnX_3$ systems. It reports the phase diagram and electrical conductivity of the $PrBr_3$−KBr binary system. The only literature information on this system was the graphic-only phase diagram reported by Blachnik and Jaeger-Kasper,[4] with no detail for the invariant points (composition/temperature).

Experimental Section

Chemicals. Praseodymium(III) bromide was synthesized from the praseodymium oxide, Pr_6O_{11}. This oxide was dissolved in hot concentrated HBr acid. The solution was evaporated, and $PrBr_3 \cdot xH_2O$ was crystallized. Ammonium bromide was then added, and this wet mixture of hydrated $PrBr_3$ and NH_4Br was first slowly heated up to 450 K and then up to 570 K to remove the water. The resulting mixture was subsequently heated to 650 K for the sublimation of NH_4Br. Finally, the salt was melted at about 1100 K. Crude $PrBr_3$ was purified by distillation under reduced pressure (≈ 0.1 Pa) in a quartz ampule at 1150 K. $PrBr_3$ prepared in this way was of a high purity, min. 99.9 %. Chemical analysis was performed by mercurimetric (bromine) and complexometric (praseodymium) methods. The results were as follows: Pr, (36.96 ± 0.15) % (37.02 % theoretical); Br, (63.04 ± 0.11) % (62.98 % theoretical).

Potassium bromide was a Merck Suprapur reagent (minimum 99.9 %). Before use, it was progressively heated up to fusion under gaseous HBr atmosphere. Excess HBr was then removed from the melt by argon bubbling.

All chemicals were handled inside a high purity argon atmosphere in a glovebox (water mass fraction $2 \cdot 10^{-6}$).

Measurements. Experimental mixture samples, made from the appropriate amounts of $PrBr_3$ and KBr, were melted in vacuum-sealed quartz ampules. The melts were homogenized and solidified. These samples were ground in an agate mortar in a glovebox. Homogenous mixtures of different compositions were prepared in this way and used in the phase diagram and electrical conductivity measurements.

Phase equilibria in the $PrBr_3$−KBr system were investigated with a Setaram DSC 121 differential scanning calorimeter (DSC). Experimental samples ((300 to 500) mg) were contained in vacuum-sealed quartz ampules. Experiments were conducted at heating and cooling rates ranging from (1 to 5) $K \cdot min^{-1}$. Because of the wide experimental temperature range, the determination of the DSC calibration constant and its evolution is crucial. This enthalpy calibration was performed by "Joule effect". It was carried out over the entire temperature range by

† Part of the "Josef M. G. Barthel Festschrift".

* To whom correspondence should be addressed. E-mail: marcelle.gaune-escard@polytech.univ-mrs.fr.
‡ Wroclaw University of Technology.
§ Ecole Polytechnique.

10.1021/je900891s
Published on Web 02/01/2010

the so-called "step method" ($\Delta T = 5$ K) and yielded the calorimeter calibration curve, that is, calorimeter constant dependence on temperature, $K(\mu V/mW) = f(T)$. This dependence was automatically used during data treatment by the original Setaram software. The sample temperature was measured by a platinum probe located in the calorimetric block. The experimental temperature scale was normalized from temperature calibration experiments performed on several standard reference materials, at various scanning rates. The resulting temperature correction coefficients were introduced into the calorimeter software.

The maximum relative experimental error on the enthalpy of phase transition did not exceed 1 %. This was controlled by the temperature and enthalpy of phase transition measurements performed on standard substances. The results obtained in this way (differences in fusion temperatures less than 1 K, differences in enthalpies of fusion less than 0.5 %) confirmed the accuracy and reproducibility of the calorimeter.

Electrical conductivity measurements were carried out in the capillary quartz cells described in details elsewhere,[5] and calibrated with molten NaCl.[6] The cell constants varied between (9500 and 11500) m^{-1}. The change of any individual cell constant was less than 1 % after several experiments. The conductivity of the melt was measured by platinum electrodes with the conductivity meter Tacussel CD 810 during increasing and decreasing temperature runs. The mean values of these two runs were used in calculations. Experimental runs were performed at heating and cooling rates of 1 $K \cdot min^{-1}$. Temperature was measured with a Pt/Pt−Rh(10) thermocouple with 1 K accuracy. Temperature and conductivity data acquisition was made with a personal computer, interfaced to the conductivity meter. All measurements were carried out under static argon atmosphere. The uncertainty of measurements was estimated at ± 2 %.

Results

Phase Diagram. DSC investigations performed on samples with different compositions yielded both the corresponding temperature and enthalpy. The enthalpy values of thermal effects obtained from heating and cooling runs were almost the same, the difference not exceeding 2 %. However, because of undercooling, all temperature and enthalpy values reported here were determined from heating curves. Solidus and liquidus temperatures were determined as T_{onset} and T_{peak} of appropriate effects, respectively.

In all thermograms, the endothermic effect at the highest temperature corresponds to liquidus. In the composition range $0 < x \leq 0.250$, where x is the molar fraction of $PrBr_3$, two additional endothermic peaks were present in all heating thermograms (except for samples of composition very close to the eutectic). The first one, at 849 K (mean value from measurements), is observable in all thermograms up to $x < 0.250$. Its disappearance for the composition $x = 0.250$ suggests the existence of the K_3PrBr_6 compound. This thermal event at 849 K can be undoubtedly ascribed to the $KBr-K_3PrBr_6$ eutectic. The eutectic composition was determined accurately from the Tamman plot[7,8] (Figure 1a). The analysis of this experimental enthalpy versus composition plot is evidence that no solid solutions form in the system. Thus, the corresponding straight lines intercept the composition axis at $x = 0$ and $x = 0.250$. The eutectic composition ($x = 0.182 \pm 0.002$) was determined from the intercept of the two linear parts in Figure 1a, described by the equations $\Delta_{fus}H_m = 71.32x$ and $\Delta_{fus}H_m/kJ \cdot mol^{-1} = 47.35 - 189.40x$ (x denotes the mole fraction of $PrBr_3$). The eutectic

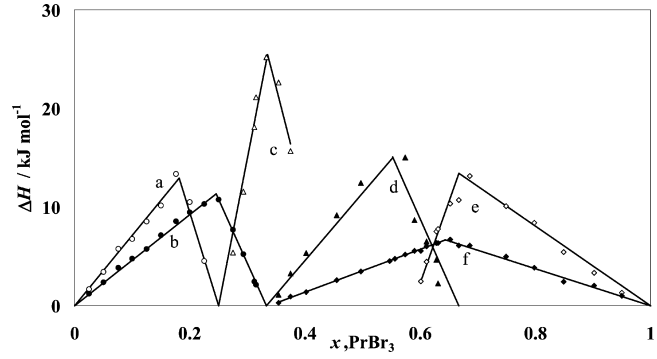

Figure 1. Experimental enthalpy vs composition Tamman plots for the $PrBr_3-KBr$ system: (a) $KBr-K_3PrBr_6$ eutectic; (b) congruently melting K_3PrBr_6 compound formation; (c) incongruently melting K_2PrBr_5 compound; (d) $K_2PrBr_5-KPr_2Br_7$ eutectic; (e) incongruently melting KPr_2Br_7 compound; (f) KPr_2Br_7 compound formation.

temperature determined from all appropriate DSC curves was found to be 849 ± 1 K, whereas the enthalpy of fusion at the eutectic composition was equal to 12.9 ± 0.3 $kJ \cdot mol^{-1}$.

The second thermal effect observed at 727 K (mean value for samples of different composition) with samples in the composition range $0 < x \leq 0.250$ is observed also in all samples with a $PrBr_3$ molar fraction up to $x < 0.333$, the composition at which it disappears. It corresponds to the formation of the K_3PrBr_6 compound (Tamman plot, Figure 1b). The molar enthalpy related to this effect (calculated for the K_3PrBr_6 compound), $\Delta_{trs}H_m = (46.9 \pm 0.4)$ $kJ \cdot mol^{-1}$, is in excellent agreement with the enthalpy observed for the formation of many M_3LnX_6 compounds (M = K, Rb; Ln = lanthanide) from the reaction between MX and M_2LnX_5.[9,10] Two thermal events observed at (727 and 904) K for a sample with the composition $x = 0.250$ are related to K_3PrBr_6 compound formation and its congruent melting, respectively.

In samples of composition $x \geq 0.333$, no effect was visible around 727 K, suggesting the existence of another compound, namely, K_2PrBr_5. Indeed, the additional thermal effect at 847 K, which appears in samples in the $PrBr_3$ composition range $0.250 < x \leq 0.375$, corresponds to the incongruent melting of K_2PrBr_5. This compound composition was confirmed by a Tamman diagram construction (enthalpy related to the effect at 847 K vs molar fraction of $PrBr_3$). The compound composition, $x = 0.335 \pm 0.019$, determined from the intercept of the two straight lines in this Figure 1c is in good agreement with the theoretical value $x = 0.333$.

Two or three endothermic peaks in addition to liquidus were observed for samples in the $PrBr_3$ composition range $0.250 < x < 1$ in heating thermograms. The first one at 847 K (as mentioned above) corresponds to the incongruent melting of K_2PrBr_5. The second one, for samples in the range $0.333 < x < 0.666$, is observable at 753 K and disappears for $x \geq 0.666$, thus suggesting the existence of another compound, namely, KPr_2Br_7. Therefore, it can be ascribed to the $K_2PrBr_5-KPr_2Br_7$ eutectic. The enthalpy related to this effect was plotted against composition in Figure 1d. The eutectic composition, $x = 0.552 \pm 0.013$, was found from the intercept of the two straight lines described by equations $\Delta_{fus}H_m/kJ \cdot mol^{-1} = -22.81 + 68.50x$ and $\Delta_{fus}H_m/kJ \cdot mol^{-1} = 87.56 - 131.20x$. The mixture with eutectic composition melts at 753 K, with enthalpy, $\Delta_{fus}H_m = (15.1 \pm 0.5)$ $kJ \cdot mol^{-1}$. In this Tamman construction it was assumed that there was no solubility in the solid state. Thus the straight lines intercept the composition axis at $x = 0.333$ and $x = 0.666$.

Table 1. DSC Results for the $PrBr_3$−KBr Binary System

	T/K						
$x(PrBr_3)$	K_3PrBr_6 formation	KBr−K_3PrBr_6 eutectic	K_2PrBr_5 decomposition	KPr_2Br_7 formation	K_2PrBr_5−KPr_2Br_7 eutectic	KPr_2Br_7 decomposition	liquidus
0.000							1007
0.024	728	848					1002
0.050	727	847					990
0.076	728	848					970
0.100	727	847					951
0.124	728	847					929
0.149	727	847					903
0.175	727	848					859
0.200	727	847					880
0.224	727	846					897
0.250	728						904
0.275	727		842				893
0.293	727		843				884
0.311	727		849				875
0.315	726		850				873
0.333			847				857
0.353			854	687	755		854
0.375			846	691	758		846
0.401				691	757		835
0.455				687	759		813
0.497				687	760		795
0.546				690	753		753
0.556				690	753		753
0.573				689	758		770
0.589				687	760		782
0.601				689	755		786
0.610				688	758		792
0.628				688	758	787	809
0.631				687	759	788	811
0.651				687	754	789	825
0.666				687		782	834
0.686				687		785	850
0.749				687		784	882
0.797				686		783	905
0.849				686		781	923
0.902				687		779	942
0.949				687		774	957
1							964

The existence of the KPr_2Br_7 compound is confirmed by the thermal effect at 786 K, which appears in mixtures of composition $0.621 \leq x(PrBr_3) < 1.0$. It is undoubtedly related to the incongruent melting of this compound. A plot of molar enthalpy related to this effect versus the molar fraction of $PrBr_3$ is presented in Figure 1e. The straight lines in this plot intercept $x = 0.667 \pm 0.025$, a value which is in excellent agreement with the theoretical stoichiometry of the KPr_2Br_7 compound (0.666).

Finally, the effect at 697 K, observable in all mixtures of composition $0.333 < x(PrBr_3) < 1.0$, corresponds either to the solid−solid phase transition or the formation of the KPr_2Br_7 compound. This suggestion comes from the Tamman plot in Figure 1f. The intercept of the straight lines in this plot yields the value $x = 0.644 \pm 0.015$, which corresponds well to the stoichiometry of the KPr_2Br_7 compound.

All of the results of the DSC investigation are presented in Table 1, and the detailed phase diagram is shown in Figure 2.

Careful analysis of heating DSC curves has showed in most cases an additional, exothermic effect in the temperature range of (430 to 518) K. These effects are also presented in Figure 2. This exothermic effect for mixtures in the $PrBr_3$ composition range 0.05 to 0.250 are undoubtedly connected with the K_3PrBr_6 compound. As earlier postulated, the effect at 727 K corresponds to K_3PrBr_6 compound formation from K_2PrBr_5 and KBr. Indeed such a formation occurs in many LnX_3−MX systems with M = K, Rb, or Cs as the result of a "reconstructive phase transition"[9] and is associated with large enthalpy changes (45 to 55) $kJ \cdot mol^{-1}$.[9,10] In solid-state reactions which are "reconstructive phase transitions", the

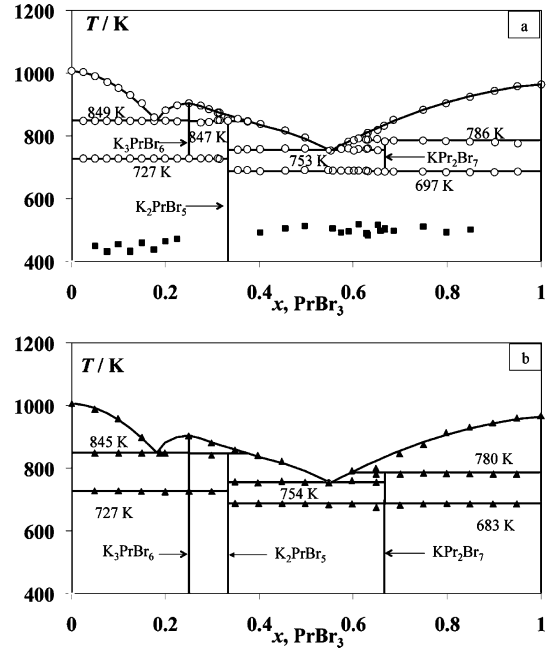

Figure 2. Phase diagram of the $PrBr_3$−KBr system: (a) this work: ○, solid lines; □, exothermic effects related to decomposition of undercooled metastable phases (K_3PrBr_6 and KPr_2Br_7); (b) literature data:[4] ▲, broken lines.

Table 2. Coefficients of the Equation $\ln \kappa = A_0 + A_1(1000/T) + A_2(1000/T)^2$ and the Activation Energy of the Electrical Conductivity (E_A) of Liquid $PrBr_3$−KBr Binary Mixtures at 1050 K[a]

	temp range	A_0	A_1	A_2			E_A at 1050 K
$x(PrBr_3)$	K	$S \cdot m^{-1}$	$S \cdot m^{-1} \cdot K$	$S \cdot m^{-1} \cdot K^2$	ln(*s*)	*n*	$kJ \cdot mol^{-1}$
0.000	1020 to 1122	5.9635	−0.3176	−0.5478	0.0008	263	11.300
0.104	980 to 1110	5.3960	0.4596	−1.0205	0.0015	320	12.339
0.195	874 to 1150	5.6503	−0.3830	−0.9131	0.0024	577	14.780
0.250	885 to 1095	4.6384	1.6648	−1.7436	0.0022	515	13.770
0.293	885 to 1110	5.2632	0.2641	−1.0691	0.0041	538	14.734
0.309	870 to 1100	4.9354	0.9686	−1.4161	0.0022	540	14.373
0.395	870 to 1150	5.1326	0.5460	−1.2579	0.0026	608	15.406
0.397	862 to 1150	5.2937	0.2942	−1.1112	0.0012	612	15.172
0.505	865 to 1150	4.7532	1.4310	−1.7975	0.0021	601	16.568
0.617	865 to 1160	4.3258	2.4769	−2.4871	0.0021	592	18.794
0.666	833 to 1080	3.1356	4.7442	−3.6334	0.0128	523	18.729
0.705	840 to 1110	3.1707	4.9365	−3.8426	0.0018	328	19.810
0.800	916 to 1110	4.1796	3.0002	−2.9680	0.0056	497	22.058
0.907	945 to 1100	3.4621	4.5336	−3.8901	0.0214	347	23.912
0.920	956 to 1110	4.3049	3.0460	−3.2837	0.0049	383	26.677
1.000	977 to 1170	4.9342	1.6942	−2.6688	0.0027	454	28.178

[a] κ is in $S \cdot m^{-1}$; ln(*s*) is the standard deviation of ln κ; *n* = number of experimental data points.

arrangement of ions is drastically changed. Ions have to move from one site to another passing through the strong potential walls of other ions. The resulting "kinetic hindrance" can cause great difference between the reaction temperatures, as measured in DSC heating and cooling runs (thermal hysteresis).[11] In extreme cases in cooling experiments, "undercooling" can become so strong that the reaction does not occur in the time-scale of DSC. Because of kinetic reasons the decomposition during cooling does not take place any longer, and the compound still exists under a metastable form. Sometimes this "undercooled" decomposition occurs abruptly during a subsequent heating run, as it was observed for K_3NdBr_6.[12] It is very likely that a similar situation takes place in the case of the K_3PrBr_6 compound. During cooling, the decomposition of this compound into K_2PrBr_5 and KBr is not completed because of kinetic reasons, and some amount of K_3PrBr_6 still exists at room temperature as a metastable phase. On a subsequent heating run, this "undercooled" decomposition occurs abruptly, and the exothermic effect corresponding to this decomposition appears in the DSC curve.

A similar hypothesis can be postulated as an explanation of the nature of exothermic effects occurring in the samples of composition $0.333 < x < 1$. It is very likely that the KPr_2Br_7 compound forms also at higher temperature during the reaction between K_2PrBr_5 and $PrBr_3$. Thus, its formation is a "reconstructive phase transition". One can assume that, similarly as in the case of K_3PrBr_6, during cooling the formation of a metastable phase of the KPr_2Br_7 compound takes place (instead of its decomposition). On a subsequent heating run this "undercooled" decomposition occurs, resulting in an exothermic effect visible on the corresponding heating DSC curve.

These results are displayed in Figure 2a. The only reference available in literature[4] was a graphic-only phase diagram that did not include any numerical data. For the sake of comparison, this diagram was digitized, and the characteristic temperatures were extracted (Figure 2b). Although three definite compounds have been also reported, the congruently melting K_3PrBr_6 and incongruently melting K_2PrBr_5 and KPr_2Br_7, the information reported by Blachnik and Jaeger-Kasper about the solid−solid phase transition in K_3PrBr_6 and KPr_2Br_7 seems incorrect. It is very likely that these compounds form at high temperature because of the "reconstructive phase transition" as explained above.

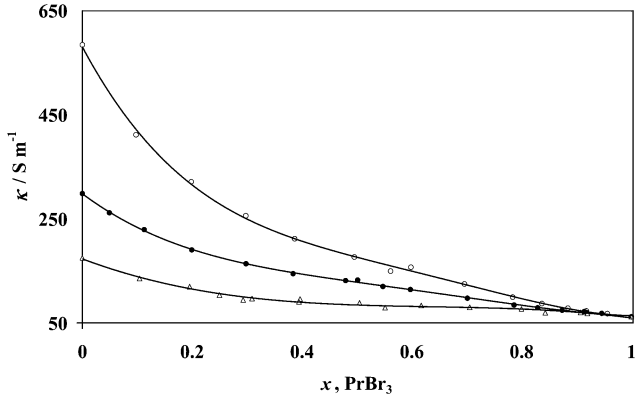

Figure 3. Electrical conductivity isotherms of $PrBr_3$−MBr liquid mixtures at 1050 K: ○, M = Li; ●, M = Na; △, M = K; solid lines, polynomial fitting.

Electrical Conductivity. The electrical conductivity of the $PrBr_3$−KBr liquid mixtures was measured for the first time. Experimental determinations were conducted over the entire composition range in steps of about $x = 0.1$ and a wide temperature range.

The experimental conductivity, κ, data of the liquid phase were fitted to the second-order equation against temperature (*T*):

$$\ln(\kappa) = A_0 + A_1\left(\frac{1000}{T}\right) + A_2\left(\frac{1000}{T}\right)^2 \quad (1)$$

where A_0, A_1, and A_2 are coefficients determined by the least-squares method. The activation energy, E_A, evaluated by analogy to the Arrhenius equation as

$$E_A(T) = -R\frac{\mathrm{d}\ln(\kappa)}{\mathrm{d}\left(\frac{1000}{T}\right)} \quad (2)$$

where *R* is the gas constant, becomes

$$E_A = -R\left[A_1 + 2A_2\left(\frac{1000}{T}\right)\right] \quad (3)$$

All A_i coefficients are listed in Table 2, together with the E_A values determined at 1050 K for all of the $PrBr_3$−KBr mixtures.

The experimental conductivity isotherm at 1050 K was plotted against the mole fraction of $PrBr_3$ in Figure 3, together with the isotherms determined earlier for the analogous systems with LiBr and NaBr.[1] It is evident that electrical conductivity

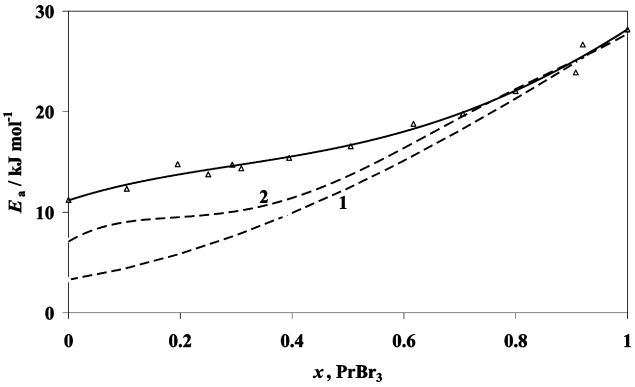

Figure 4. Activation energy at 1050 K of $PrBr_3$−MBr liquid mixtures: broken line 1, M = Li; broken line 2, M = Na; △, M = K; solid line, polynomial fitting, M = K.

decreases with the increasing radius of the alkali metal cation, that is, from lithium to potassium. This conductivity decreases also with the increase of $PrBr_3$ concentration, with significantly larger changes in the alkali bromide-rich region. A similar trend has been already observed in our previous investigations of lanthanide halide−alkali metal halide binary systems.[13−15]

As indicated above, the activation energy for conductivity changes with temperature, validating the early statement made by Yaffe and Van Artsdalen[16,17] of a correlation with structural changes in melting. Figure 4 shows the activation energy at 1050 K as function of the composition. For comparison, the data on activation energy for the analogous systems with LiBr and NaBr[1] are also included in Figure 4. A stabilization effect of E_A, although somewhat unclear, seems to occur in the range (25 to 50) mol % of $PrBr_3$ for the systems with NaBr and KBr. This effect can be explained[11,13] as consistent with the predominant $LnBr_6^{3-}$ octahedral complexes in the KBr-, RbBr- and CsBr-rich melts, with an increasing amount of polymeric species in the $LnBr_3$-rich melts.

Figure 4 clearly illustrates also that the activation energy increases with the alkali cationic radius particularly in the MBr-rich melts. It is likely that this is due to an increase of the $PrBr_6^{3-}$ complex concentration in the melt. The radius of the alkali metal cation will therefore govern the complex ion formation in the $PrBr_3$−MBr binary systems. Thus the addition of KBr to $PrBr_3$ favors complex ion formation more than NaBr and results in a larger activation energy for electrical conductivity.

Conclusions

Three stoichiometric compounds, namely, K_3PrBr_6, K_2PrBr_5, and $KbPr_2Br_7$, exist in the $PrBr_3$−KBr binary system. K_3PrBr_6 forms at 727 K and melts congruently at 904 K. K_2PrBr_5 melts incongruently at 847 K, and finally KPr_2Br_7 forms at 697 K and melts incongruently at 786 K.

The specific electrical conductivity of $PrBr_3$−KBr liquid mixtures is indicative of $PrBr_6^{3-}$ octahedral complexes formation in melting.

Literature Cited

(1) Ingier-Stocka, E.; Rycerz, L.; Berkani, M.; Gaune-Escard, M. Thermodynamic and transport properties of the $PrBr_3$-MBr Binary Systems (M = Li, Na). *J. Mol. Liq.* **2009**, *148* (1), 40–44.

(2) Seifert, H. J. Ternary Chlorides of the Trivalent Late Lanthanides. Phase diagrams, crystal structures and thermodynamic properties. *J. Therm. Anal. Calorim.* **2006**, *83* (2), 479–505, and references therein.

(3) Cock, L. P.; McMurdie, H. F. Phase Diagrams for Ceramists. *J. Am. Ceram. Soc.* **1989**, *7*, 166.

(4) Blachnik, R.; Jaeger-Kasper, A. Zustandiagramme von Alkalibromid-Lanthanoid(III)-bromid-Mischungen. *Z. Anorg. Allg. Chem.* **1980**, *461*, 74–86.

(5) Fouque, Y.; Gaune-Escard, M.; Szczepaniak, W.; Bogacz, A. Synthèse, mesures des conductibilitiés électriques et des entropies de changements d′états pour le composé Na_2Ubr_6. *J. Chim. Phys.* **1978**, *75*, 361–366.

(6) Janz, G. J. Thermodynamic and Transport Properties for Molten Salts; Correlation Equations for Critically Evaluated Density, Surface tension, Electrical Conductance, and Viscosity Data. *J. Phys. Chem. Ref. Data* **1988**, *2*, 17.

(7) Findlay, A. *The phase rule and its applications*; Longmans, Green and Co.: New York, 1911.

(8) Desch C. H., *Intermetallic compounds*, Longmans, Green and Co., New York, Bombay and Calcutta, 1914.

(9) Rycerz, L. High Temperature Characterization of LnX_3 and LnX_3-AX Solid and Liquid Systems (Ln = Lanthanide, A = Alkali, X = Halide). Thermodynamics and Electrical Conductivity. Ph.D. Thesis, Universite de Provence Aix-Marseille I, France, Marseille, 2003.

(10) Rycerz, L. Thermochemistry of lanthanide halides and compounds formed in lanthanide halide-alkali metal halide systems (in Polish). *Scientific Papers of Institute of Inorganic Chemistry and Metallurgy of Rare Elements*; Series Monographs 35; Wroclaw University of Technology: Wroclaw, Poland, 2004.

(11) Seifert, H. J. Ternary Chlorides of the Trivalent Early Lanthanides. Phase diagrams, crystal structures and thermodynamic properties. *J. Therm. Anal. Calorim.* **2002**, *7*, 789–826.

(12) Rycerz, L.; Gaune-Escard, M. Enthalpy of phase transitions and heat capacity of compounds formed in the $NdBr_3$ - MBr systems (M = K, Rb, Cs). *Prog. Molten Salt Chem.* **2000**, *1*, 461–465.

(13) Gadzuric, S.; Ingier-Stocka, E.; Rycerz, L.; Gaune-Escard, M. Electrical conductivity of molten binary $NdBr_3$-alkali bromide mixtures. *Z. Naturforsch.* **2004**, *59a*, 77–83.

(14) Potapov, A.; Rycerz, L.; Gaune-Escard, M. Electrical conductivity of molten rare earth chlorides. Pure chlorides and binary mixtures. *International Symposium on Ionic Liquids. Proceedings in honour of Marcelle Gaune-Escard.* Øye, H. A. Jagtoyen, A., Eds.; Carry le Rouet, France, June 26−28, 2003; pp 469−475.

(15) Ziolek, B.; Rycerz, L.; Gadzuric, S.; Ingier-Stocka, E.; Gaune-Escard, M. Electrical conductivity of molten $LaBr_3$ and $LaBr_3$-MBr binary mixtures. *Z. Naturforsch.* **2005**, *60a*, 75–80.

(16) Van Artsdalen, E. R.; Yaffe, J. S. Electrical conductance and density of molten salt systems: KCl-LiCl, KCl-NaCl and KCl-KI. *J. Phys. Chem.* **1955**, *59*, 118–27.

(17) Yaffe, J. S.; Van Artsdalen, E. R. Electrical conductance and density of pure molten alkali halides. *J. Phys. Chem.* **1956**, *60*, 1125–31.

Received for review October 26, 2009. Accepted January 16, 2010. Financial support by the Polish Ministry of Science and Higher Education from budget on science in 2007 to 2010 under the Grant No. N204 4098 33 is gratefully acknowledged. L.R. and E.I.-S. wish to thank the Ecole Polytechnique de Marseille for hospitality and support during this work.

JE900891S